

Ligand Effect on the Insertion Reactions of Allenes with $MHCl(CO)(PPh_3)_3$ and $MHCl(PPh_3)_3$ ($M = Ru, Os$)

Tao Bai,[†] Jun Zhu,[‡] Peng Xue,[‡] Herman Ho-Yung Sung,[‡] Ian Duncan Williams,[‡]
Shengming Ma,^{*,†} Zhenyang Lin,^{*,‡} and Guochen Jia^{*,‡}

State Key Laboratory of Organometallic Chemistry, Shanghai Institute of Organic Chemistry, Chinese Academy of Sciences, 354 Fenglin Lu, Shanghai 200032, People's Republic of China, and Department of Chemistry, The Hong Kong University of Science and Technology, Clear Water Bay, Kowloon, Hong Kong, People's Republic of China

Received June 23, 2007

Treatment of $RuHCl(CO)(PPh_3)_3$ with $CH_2=C=CHCO_2Me$ gives the allyl complex $Ru(\eta^3-CH_2-CHCHCO_2Me)Cl(CO)(PPh_3)_2$. The analogous allyl complexes $Os(\eta^3-CH_2CHCHR)Cl(CO)(PPh_3)_2$ ($R = Ph, CH_2Ph$) are also produced from the reactions of $OsHCl(CO)(PPh_3)_3$ with $CH_2=C=CHR$. In contrast, $MHCl(PPh_3)_3$ ($M = Ru, Os$) react with $CH_2=C=CHR$ to give the vinyl complexes $MCl(C(CH_3)=CHR)-(CH_2=C=CHR)(PPh_3)_2$ ($M = Ru, R = CMe_3, M = Os, R = CMe_3, Ph, CO_2Et$). The difference in the reaction pathways for the reactions of allenes with $MHCl(CO)(PPh_3)_3$ and $MHCl(PPh_3)_3$ ($M = Ru, Os$) has been studied by computational chemistry. The theoretical study shows that the observed different reactivity can be related to the significant difference in the electron density increase at the central carbon of the allene ligand upon coordination to the metal fragments.

Introduction

Transition metal-catalyzed reactions of allenes have found increasing applications in organic and polymer synthesis.^{1,2} In many of the catalytic reactions of allenes, insertion of allenes into $M-R$ bonds is one of the most important fundamental steps. Allene insertion reactions with L_nM-R complexes can, in principle, give either transition metal allyl complexes **A** or vinyl complexes **B** as illustrated in eq 1. The insertion of allenes into $M-R$ bonds to give allyl intermediates **A** has been frequently invoked in the mechanisms of transition metal-catalyzed reactions of allenes. In support of the proposed mechanisms, stoichiometric insertion reactions of allenes with mononuclear complexes L_nM-R (e.g., $M = Ni,$ ³ $Pd,$ ⁴ $Pt,$ ⁵ $Co,$ ⁶ $Rh,$ ⁷ $Ir,$ ^{7d} $Fe,$ ⁸ $Ru,$ ⁹ $Mo,$ ¹⁰ $Ta,$ ¹¹ $Zr,$ ¹² $Hf,$ ¹³ $R = H,$ acyl, allyl, vinyl, alkyl,

and aryl) to give transition metal allyl complexes are now well documented.

(3) (a) Hoberg, H.; Heger, G.; Kruger, C.; Tsay, Y. H. *J. Organomet. Chem.* **1988**, *348*, 261. (b) Hoberg, H.; Fanaanas, F. *J. Angew. Chem., Int. Ed. Engl.* **1985**, *24*, 325. (c) Baker, R.; Copeland, A. H. *J. Chem. Soc., Perkin Trans.* **1977**, 2560, and references therein.

(4) (a) Sirlin, C.; Chengebroyen, J.; Konrath, R.; Ebeling, G.; Raad, I.; Dupont, J.; Paschaki, M.; Kotzyba-Hibert, F.; Harf-Monteil, C.; Pfeffer, M. *Eur. J. Org. Chem.* **2004**, 1724. (b) Canovese, L.; Visentin, F.; Chessa, G.; Uguagliati, P.; Santo, C.; Bandoli, G.; Maini, L. *Organometallics* **2003**, *22*, 3230. (c) Chengebroyen, J.; Linke, M.; Robitzer, M.; Sirlin, C.; Pfeffer, M. *J. Organomet. Chem.* **2003**, *687*, 313. (d) Canovese, L.; Chessa, G.; Santo, C.; Visentin, F.; Uguagliati, P. *Inorg. Chim. Acta* **2003**, *346*, 158. (e) Yagyu, T.; Suzuki, Y.; Osakada, K. *Organometallics* **2002**, *21*, 2088. (f) Canovese, L.; Visentin, F.; Chessa, G.; Santo, C.; Uguagliati, P. *J. Organomet. Chem.* **2002**, *650*, 43. (g) Yagyu, T.; Hamada, M.; Osakada, K.; Yamamoto, T. *Organometallics* **2001**, *20*, 1087. (h) Canovese, L.; Visentin, F.; Chessa, G.; Uguagliati, P.; Bandoli, G. *Organometallics* **2000**, *19*, 1461. (i) Devisi, A.; Edwards, P. G.; Newman, P. D.; Toose, R. P. *Dalton Trans.* **2000**, 523. (j) Delis, J. G. P.; Groen, J. H.; Vrieze, K.; van Leeuwen, P. W. N. M.; Veldman, N.; Spek, A. L. *Organometallics* **1997**, *16*, 551. (k) Kacker, S.; Sen, A. *J. Am. Chem. Soc.* **1997**, *119*, 10028. (l) Groen, J. H.; Elsevier, C. J.; Vrieze, K.; Smeets, W. J. J.; Spek, A. L. *Organometallics* **1996**, *15*, 3445. (m) Ankersmit, H. A.; Loken, B. H.; Kooijman, H.; Spek, A. L.; Vrieze, K.; van Koten, G. *Inorg. Chim. Acta* **1996**, *252*, 141. (n) Ankersmit, H. A.; Veldman, N.; Spek, A. L.; Eriksen, K.; Goubitz, K.; Vrieze, K.; van Koten, G. *Inorg. Chim. Acta* **1996**, *203*. (o) Chengebroyen, J.; Pfeffer, M.; Sirlin, C. *Tetrahedron Lett.* **1996**, *40*, 7263. (p) De Felice, V.; Cucciolito, M. E.; De Renzi, A.; Ruffo, F.; Tesaro, D. *J. Organomet. Chem.* **1995**, *493*. (q) Rulke, R.; Kliphuis, D.; Elsevier, C. J.; Fraanje, J.; Goubitz, K.; Leeuwen, P. W. N. M.; Vrieze, K. *J. Chem. Soc. Chem. Commun.* **1994**, 1817. (r) May, C. J.; Powell, J. J. *Organomet. Chem.* **1980**, *184*, 385. (s) Hughes, R. P.; Powell, J. J. *Organomet. Chem.* **1973**, *60*, 409. (t) Okamoto, T. *Bull. Chem. Soc. Jpn.* **1971**, *44*, 1353. (u) Okamoto, T. *Bull. Chem. Soc. Jpn.* **1970**, *43*, 2658. (v) Medema, D.; van Helden, R.; Kohll, C. F. *Inorg. Chim. Acta* **1969**, *3*, 255. (w) Lupin, M. S.; Shaw, B. L. *J. Chem. Soc. (A)* **1966**, 1687. (x) Schultz, R. G. *Tetrahedron* **1964**, *20*, 2809.

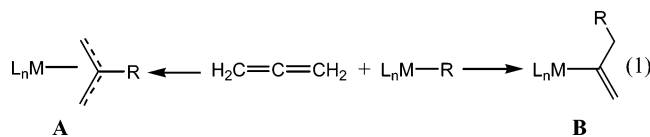
(5) (a) Clark, H. C.; Milne, C. R. C.; Wong, C. S. *J. Organomet. Chem.* **1977**, *136*, 265. (b) Ros, R.; Michelin, R. A.; Bataillard, R.; Roulet, R. *J. Organomet. Chem.* **1979**, *165*, 107. (c) Chisholm, M. H.; Johns, W. S. *Inorg. Chem.* **1975**, *14*, 1189. (d) Chisholm, M. H.; Clark, H. C. *Inorg. Chem.* **1973**, *12*, 991. (e) Deeming, A. J.; Johnson, B. F. G.; Lewis, J. J. *Chem. Soc., Dalton Trans.* **1973**, 1848. (f) C. Clark H. C.; Kurosawa, H. *Inorg. Chem.* **1972**, *11*, 1275. (g) Chisholm, M. H.; Clark, H. C.; Hunter, D. H. *Chem. Commun.* **1971**, 809. (h) Deeming, A. J.; Johnson, B. F. G.; Lewis, J. *Chem. Soc. D.: Chem. Commun.* **1970**, 598. (i) ref. 4p.

[†] Shanghai Institute of Organic Chemistry.

[‡] The Hong Kong University of Science and Technology.

(1) (a) Ma, S. *Chem. Rev.* **2005**, *105*, 2829. (b) Hong, S.; Marks, T. J. *Acc. Chem. Res.* **2004**, *37*, 673. (c) Sydnese, L. K. *Chem. Rev.* **2003**, *103*, 1133. (d) Ma, S. *Acc. Chem. Res.* **2003**, *36*, 701. (e) Zimmer, R.; Dinesh, C. U.; Nandan, E.; Khan, F. A. *Chem. Rev.* **2000**, *100*, 3067.

(2) Examples of recent work: (a) Ma, S.; Zheng, Z.; Jiang, X. *Org. Lett.* **2007**, *9*, 529. (b) Chang, H.-T.; Jayanth, T. T.; Cheng, C.-H. *J. Am. Chem. Soc.* **2007**, *129*, 4166. (c) Buzas, A. K.; Istrate, F. M.; Gagosz, F. *Org. Lett.* **2007**, *9*, 985. (d) LaLonde, R. L.; Sherry, B. D.; Kang, E. J.; Toste, F. D. *J. Am. Chem. Soc.* **2007**, *129*, 2452. (e) Chen, G.; Fu, C.; Ma, S. *J. Org. Chem.* **2006**, *71*, 9877. (f) Ma, S.; Guo, H.; Yu, F. *J. Org. Chem.* **2006**, *71*, 6634. (g) Reynolds, T. E.; Bharadwaj, A. R.; Scheidt, K. A. *J. Am. Chem. Soc.* **2006**, *128*, 15382. (h) Regas, D.; Ruiz, J. M.; Afonso, M. M.; Palenzuela, J. A. *J. Org. Chem.* **2006**, *71*, 9153. (i) Kino, T.; Taguchi, M.; Tazawa, A.; Tomita, I. *Macromolecules* **2006**, *39*, 7474. (j) Ohmura, T.; Taniguchi, H.; Sugimoto, M. *J. Am. Chem. Soc.* **2006**, *128*, 13682. (k) Bayden, A. S.; Brummond, K. M.; Jordan, K. D. *Organometallics* **2006**, *25*, 5204. (l) Gockel, B.; Krause, N. *Org. Lett.* **2006**, *8*, 4485. (m) Pelz, N. F.; Morken, J. P. *Org. Lett.* **2006**, *8*, 4557. (n) Mochizuki, K.; Tomita, I. *Macromolecules* **2006**, *39*, 6336. (o) Trost, B. M.; McClory, A. *Org. Lett.* **2006**, *8*, 3627. (p) Liu, Z.; Wasmuth, A. S.; Nelson, S. G. *J. Am. Chem. Soc.* **2006**, *128*, 10352. (q) Zhang, Z.; Liu, C.; Kinder, R. E.; Han, X.; Qian, H.; Widenhofer, R. A. *J. Am. Chem. Soc.* **2006**, *128*, 9066. (r) Barluenga, J.; Vicente, R.; Lopez, L. A.; Tomas, M. *J. Am. Chem. Soc.* **2006**, *128*, 7050. (s) Lee, P. H.; Lee, K.; Kang, Y. *J. Am. Chem. Soc.* **2006**, *128*, 1139. (t) Sieber, J. D.; Morken, J. P. *J. Am. Chem. Soc.* **2006**, *128*, 74.



In contrast, examples of stoichiometric insertion of allenes into M–R bonds to give vinyl complexes **B** are still very rare, although such a reaction may also occur in metal-catalyzed reactions of allenes.¹⁴ Stoichiometric reactions of allenes with binuclear hydrido/alkyl complexes to give vinyl complexes have been observed occasionally.^{15,16} As rare examples of formation of vinyl complexes from the insertion reactions of allenes with mononuclear complexes $\text{L}_n\text{M}-\text{R}$, Hills et al. reported that $[\text{FeH}(\text{H}_2)(\text{dmpe})_2]^+$ reacts with $\text{CH}_2=\text{C}=\text{CH}_2$ to give the vinyl complex $[\text{Fe}(\text{C}(\text{CH}_3)=\text{CH}_2)(\text{dmpe})_2]^+$;¹⁷ Jordan et al. showed that $[\text{Cp}_2\text{Zr}(\eta^2\text{-pyridyl})(\text{THF})]^+$ reacts with allene to give a

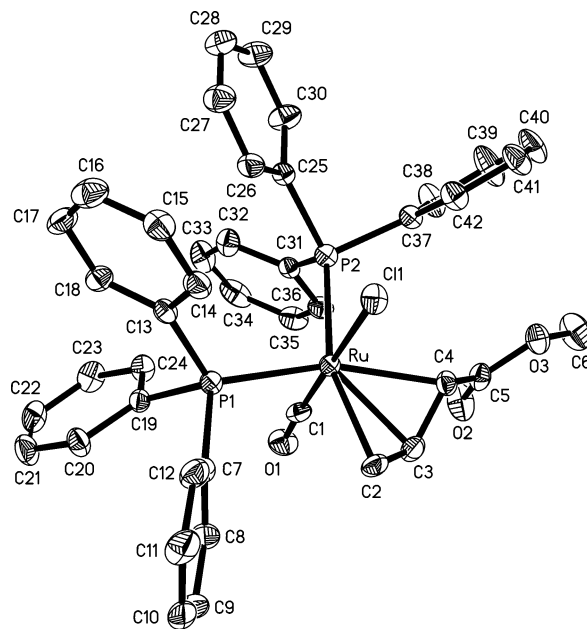


Figure 1. X-ray structure of $\text{Ru}(\eta^3\text{-CH}_2\text{CHCHC}(\text{O})\text{OMe})\text{Cl}(\text{CO})(\text{PPh}_3)_2$ (**2**).

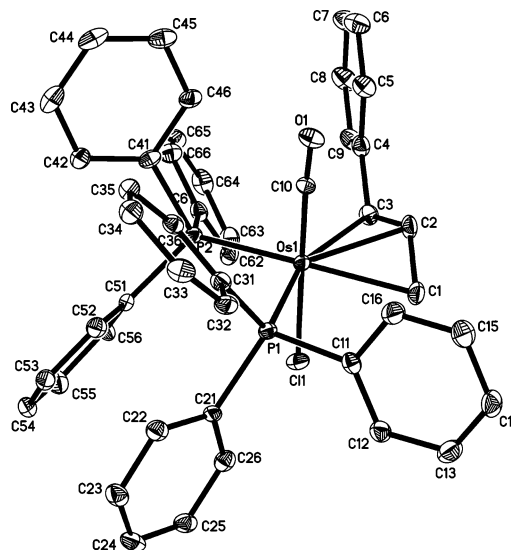


Figure 2. X-ray structure of $\text{Os}(\eta^3\text{-CH}_2\text{CHCHPh})\text{Cl}(\text{CO})(\text{PPh}_3)_2$ (**4**).

mixture of vinyl and allyl complexes;¹⁸ Erker et al. reported that $\text{Cp}_2\text{M}(\text{CH}_2\text{CHCHCH}_2\text{B}(\text{C}_6\text{F}_5)_3)$ ($\text{M} = \text{Zr}, \text{Hf}$) react with allene to give the vinyl complexes $\text{Cp}_2\text{M}(\text{C}(\text{C}=\text{CH}_2)\text{CH}_2\text{CH}_2\text{-CHCHCH}_2\text{B}(\text{C}_6\text{F}_5)_3)$.¹⁹ One may wonder why formation of allyl complexes prevails over vinyl complexes in the majority of allene insertion reactions and how one can tune the properties of $\text{L}_n\text{M}-\text{R}$ so that they undergo insertion reactions with allenes to give vinyl complexes rather than allyl complexes. The answers to these questions may help to develop new catalytic reactions of allenes.

This work concerns allene insertion reactions of $\text{MHCl}(\text{PPh}_3)_3$ ($\text{M} = \text{Ru}, \text{Os}$) and $\text{MHCl}(\text{CO})(\text{PPh}_3)_3$ ($\text{M} = \text{Ru}, \text{Os}$). The reactions of $\text{RuHCl}(\text{CO})(\text{PPh}_3)_3$ with simple allenes such as $\text{CH}_2=\text{C}=\text{CH}_2$, $\text{CH}_2=\text{C}=\text{CHPh}$ and $\text{CH}_2=\text{C}=\text{CMe}_2$ have been reported to give η^3 -allyl complexes.⁹ Interestingly, the osmium hydride complex $\text{OsHCl}(\text{PPh}_3)_3$ reacts with $\text{CH}_2=\text{C}=\text{CHR}$ (R

(6) (a) Huo, C. F.; Li, Y. W.; Beller, M.; Jiao, H. *Chem.-Eur. J.* **2005**, *11*, 889. (b) Sovago, J.; Newton, M. G.; Mushina, E. A.; Ungvary, F. *J. Am. Chem. Soc.* **1996**, *118*, 9589.

(7) (a) Choi, J.; Osakada, K.; Yamamoto, T. *Organometallics* **1998**, *17*, 3044. (b) Osakada, K.; Choi, J. C.; Yamamoto, T. *J. Am. Chem. Soc.* **1997**, *119*, 12390. (c) Osakada, K.; Choi, J. C.; Koizumi, T.; Yamaguchi, I.; Yamamoto, T. *Organometallics* **1995**, *14*, 4962. (d) Clement, D. A.; Nixon, J. F.; Wilkins, B. *J. Organomet. Chem.* **1972**, *37*, C43. (e) Brown, C. K.; Mowat, W.; Yagupsky, G.; Wilkinson, G. *J. Chem. Soc. (A)* **1971**, 850.

(8) (a) Itoh, K.; Nakanishi, S.; Takata, T. *Chem. Lett.* **2000**, 672. (b) Roustan, J. L.; Guinot, A.; Cadiot, P. *J. Organomet. Chem.* **1980**, *194*, 357. (c) Roustan, J. L.; Merour, J. Y.; Charrier, C.; Benaim, J.; Cadiot, P. *J. Organomet. Chem.* **1979**, *168*, 61.

(9) (a) Sasabe, H.; Kihara, N.; Mizuno, K.; Ogawa, A.; Takata, T. *Chem. Lett.* **2006**, *35*, 212. (b) Xue, P.; Bi, S.; Sung, H. H. Y.; Williams, I. D.; Lin, Z.; Jia, G. *Organometallics* **2004**, *23*, 4735. (c) Sasabe, H.; Nakanishi, S.; Takata, T. *Inorg. Chem. Commun.* **2003**, *6*, 1140. (d) Sasabe, H.; Nakanishi, S.; Takata, T. *Inorg. Chem. Commun.* **2002**, *5*, 177. (e) Nakanishi, S.; Sasabe, H.; Takata, T. *Chem. Lett.* **2000**, 1058. (f) Hill, A. F.; Ho, C. T.; Wilton-Ely, D. E. T. *Chem. Commun.* **1997**, 2207.

(10) (a) Huang, B. C.; Wu, I. Y.; Lin, Y. C.; Peng, S. M.; Lee, G. H. *J. Chem. Soc., Dalton Trans.* **1995**, 2351. (b) Collin, J.; Roustan, J. L.; Cadiot, P. *J. Organomet. Chem.* **1979**, *169*, 53.

(11) Weinert, C. S.; Fanwick, P. E.; Rothwell, I. P. *Organometallics* **2005**, *24*, 5759.

(12) (a) Wipf, P.; Pierce, J. G. *Org. Lett.* **2005**, *7*, 3537. (b) Horton, A. D. *Organometallics* **1992**, *11*, 3271. (c) Jordan, R. F.; Lapointe, R. E.; Bradley, P. K.; Baenziger, N. *Organometallics* **1989**, *8*, 2892.

(13) Bercaw, J. E.; Moss, J. R. *Organometallics* **1992**, *11*, 639.

(14) (a) Stubbert, B. D.; Marks, T. J. *J. Am. Chem. Soc.* **2007**, *129*, 4253. (b) Chakravarty, M.; Kumara Swamy, K. C. *J. Org. Chem.* **2006**, *71*, 9128. (c) Hong, S.; Marks, T. J. *Acc. Chem. Res.* **2004**, *37*, 673. (d) Fu, C.; Ma, S. *Org. Lett.* **2005**, *7*, 1605. (e) Arredondo, V. M.; McDonald, F. E.; Marks, T. J. *Organometallics* **1999**, *18*, 1949. (f) Arredondo, V. M.; Tian, S.; McDonald, F. E.; Marks, T. J. *J. Am. Chem. Soc.* **1999**, *121*, 3633–3639. (g) Arredondo, McDonald, F. E.; Marks, T. J. *J. Am. Chem. Soc.* **1998**, *120*, 4871.

(15) Examples of reactions of binuclear complexes with allenes giving vinyl complexes or both vinyl and allyl complexes: (a) Chokshi, A.; Rowsell, B. D.; Trepanier, S. J.; Ferguson, M. J.; Martin, C. *Organometallics* **2004**, *23*, 4759. (b) Sterenberg, B. T.; McDonald, R.; Cowie, M. *Organometallics* **1997**, *16*, 2297. (c) Hogarth, G.; Lavender, M. H. *J. Chem. Soc., Dalton Trans.* **1992**, 2759. (d) Andrew, D.; Horton, M.; Mays, J. *J. Chem. Soc., Dalton Trans.* **1990**, 155. (e) Fontaine, X. L. R.; Jacobsen, G. B.; Shaw, B. L.; Thornton-Pett, M. *J. Chem. Soc., Dalton Trans.* **1988**, 1185.

(16) Examples of reactions of binuclear complexes with allenes giving allyl complexes only: (a) Dennett, J. N. L.; Jacke, J.; Nilsson, G.; Rosborough, A.; Ferguson, M. J.; Wang, M.; McDonald, R. Josef Takats, *J. Organometallics* **2004**, *23*, 4478. (b) Knox, S. A. R.; Morton, D. A. V.; Orpen, A. G.; Turner, M. L. *Inorg. Chim. Acta* **1994**, *220*, 201. (c) Caffyn, A. J. M.; Mays, M. J.; Solan, G. A.; Conole, G.; Tiripicchio, A. *J. Chem. Soc., Dalton Trans.* **1993**, 2345. (d) Chetcuti, M. J.; Fanwick, P. E.; Grant, B. E. *Organometallics* **1991**, *10*, 3003. (e) Conole, G.; Henrick, K.; McPartin, M.; Horton, A. D.; Mays, M. J.; Sappa, E. *J. Chem. Soc., Dalton Trans.* **1990**, 2367. (f) Autmann, R.; Melchers, H. D.; Weidenhaupt, H. *J. Chem. Ber.* **1990**, *123*, 351. (g) Autmann, R.; Weidenhaupt, H. *J. Chem. Ber.* **1987**, *120*, 105. (h) Kuhn, A.; Burschka, C.; Werner, H. *Organometallics* **1982**, *1*, 449, and references therein.

(17) Hills, A.; Hughes, D. L.; Jimenez-Tenorio, M.; Leigh, G. J.; McGeary, C. A.; Rowley, A. T.; Bravo, M.; McKenna, C. E.; McKenna, M. C. *J. Chem. Soc., Chem. Commun.* **1991**, 522.

(18) Guram, A. S.; Jordan, R. F. *Organometallics* **1991**, *10*, 3470.

(19) Karl, J.; Erker, G. *Chem. Ber.* **1997**, *120*, 1261.

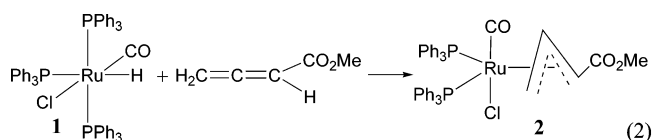
Table 1. Crystal Data and Structure Refinement for $\text{Ru}(\eta^3\text{-CH}_2\text{CHCHCO}_2\text{Me})\text{Cl}(\text{CO})(\text{PPh}_3)_2$ (2**) and $\text{Os}(\eta^3\text{-CH}_2\text{CHCHPh})\text{Cl}(\text{CO})(\text{PPh}_3)_2$ (**4**)**

	2	4
empirical formula	$\text{C}_{42}\text{H}_{37}\text{ClO}_3\text{P}_2\text{Ru}$	$\text{C}_{46}\text{H}_{39}\text{ClO}_3\text{OsP}_2$
fw	788.18	895.36
wavelength, Å	0.71073	0.71073
cryst syst	monoclinic	monoclinic
space group	$P2(1)/n$	$P2(1)/n$
<i>a</i> , Å	18.0573(14)	15.3034(9)
<i>b</i> , Å	10.1691(8)	10.0384(6)
<i>c</i> , Å	19.5850(15)	24.8593(14)
β , deg	98.765(2)	106.2710(10)
volume, Å ³	3554.3(5)	3666.0(4)
<i>Z</i>	4	4
density (calcd), Mg/m ³	1.473	1.622
absorp coeff, mm ⁻¹	0.646	3.675
<i>F</i> (000)	1616	1784
θ range, deg	2.26 to 26.00	1.41 to 24.99
no. of reflns collected	18 831	24 570
no. of indep reflns	6910 [<i>R</i> (int) = 0.0920]	6214 [<i>R</i> (int) = 0.0310]
max. and min. transmn	1.00 and 0.82	1.00 and 0.80
no. of data/restraints/params	6910/0/443	6214/0/460
goodness-of-fit on <i>F</i> ²	1.009	0.987
final <i>R</i> indices [<i>I</i> > 2 σ (<i>I</i>)]	<i>R</i> 1 = 0.0448, <i>wR</i> 2 = 0.0777	<i>R</i> 1 = 0.0194, <i>wR</i> 2 = 0.0409
largest diff peak/hole, e Å ⁻³	0.619/−0.477	0.889/−0.398

= CMe_3 , Ph, CO_2Et) to give the vinyl complexes $\text{OsCl}(\text{C}(\text{CH}_3)=\text{CHR})(\text{CH}_2=\text{C}=\text{CHR})(\text{PPh}_3)_2$ rather than the usually observed allyl complexes.²⁰ It is not clear whether the different pathways for the reactions are due to the effect of metals or ligands. To address this question, we have studied the insertion reactions of allenens with $\text{RuHCl}(\text{PPh}_3)_3$ and $\text{OsHCl}(\text{CO})(\text{PPh}_3)_3$. The insertion reaction pathways have also been investigated by computational chemistry, in order to understand the experimental observations.

Results and Discussion

Insertion Reactions of Allenens with $\text{MHCl}(\text{CO})(\text{PPh}_3)_3$ (*M* = Ru, Os) Forming Allyl Complexes. The reactions of $\text{RuHCl}(\text{CO})(\text{PPh}_3)_3$ with simple allenens such as $\text{CH}_2=\text{C}=\text{CH}_2$, $\text{CH}_2=\text{C}=\text{CHPh}$, and $\text{CH}_2=\text{C}=\text{CMe}_2$ have been shown previously to give allyl complexes $\text{RuCl}(\eta^3\text{-allyl})(\text{CO})(\text{PPh}_3)_2$. In order to further study the effect of substituents of allenens on the reaction pathway, we have studied the reaction of $\text{RuHCl}(\text{CO})(\text{PPh}_3)_3$ (**1**) with $\text{CH}_2=\text{C}=\text{CHCO}_2\text{Me}$, which has the electron-withdrawing group CO_2Me . The reaction was found also to give the allyl complex $\text{Ru}(\eta^3\text{-CH}_2\text{CHCHCO}_2\text{Me})\text{Cl}(\text{CO})(\text{PPh}_3)_2$ (**2**) (eq 2). Complex **2** must have a structure similar to that of other reported complexes $\text{Ru}(\eta^3\text{-allyl})\text{Cl}(\text{CO})(\text{PPh}_3)_2$ as inferred from the NMR data. The presence of the $\eta^3\text{-allyl}$ ligand is indicated by the ¹³C-¹H and ¹H NMR spectra. In the ¹H NMR spectrum, the central allylic proton signal was observed at 5.80 ppm, and the terminal allylic proton signals were observed in the region 2.95–3.19 ppm. The ¹³C{¹H} NMR spectrum showed the three allylic signals at 103.5, 67.8, and 60.7 ppm. The ³¹P{¹H} NMR spectrum of **2** showed two doublets at 39.5 and 28.9 ppm, due to the unsymmetrical nature of the allyl ligand.



The structure of **2** has been confirmed by an X-ray diffraction study. The molecular structure of **2** is shown in Figure 1. The

Table 2. Bond Lengths (Å) and Angles (deg) for $\text{Ru}(\eta^3\text{-CH}_2\text{CHCHCO}_2\text{Me})\text{Cl}(\text{CO})(\text{PPh}_3)_2$ (2**)**

Ru–C(1)	1.835(5)	Ru–C(2)	2.247(4)
Ru–C(3)	2.202(4)	Ru–C(4)	2.248(4)
Ru–P(1)	2.4012(12)	Ru–P(2)	2.411(12)
Ru–Cl(1)	2.4598(11)	O(1)–C(1)	1.141(5)
C(2)–C(3)	1.402(6)	C(3)–C(4)	1.421(6)
C(4)–C(5)	1.481(6)		
C(1)–Ru–C(2)	95.88(19)	C(1)–Ru–C(3)	80.82(19)
C(1)–Ru–C(4)	97.12(18)	C(1)–Ru–P(1)	88.84(15)
C(1)–Ru–P(2)	92.12(14)	C(1)–Ru–Cl(1)	178.35(14)
C(2)–Ru–C(3)	36.72(16)	C(2)–Ru–C(4)	66.72(16)
C(2)–Ru–P(1)	90.87(12)	C(2)–Ru–P(2)	160.50(13)
C(2)–Ru–Cl(1)	83.89(12)	C(3)–Ru–C(4)	37.24(16)
C(3)–Ru–P(1)	123.63(13)	C(3)–Ru–P(2)	128.40(14)
C(3)–Ru–Cl(1)	95.75(13)	C(4)–Ru–P(1)	157.23(12)
C(4)–Ru–P(2)	94.68(12)	C(4)–Ru–Cl(1)	83.41(12)
P(1)–Ru–P(2)	107.08(4)	P(1)–Ru–Cl(1)	90.08(4)
Ru–C(1)–Cl(1)	89.39(4)	Ru–C(2)–C(3)	69.9(3)
Ru–C(3)–C(2)	73.4(3)	Ru–C(3)–C(4)	73.1(2)
Ru–C(4)–C(3)	69.6(2)	Ru–C(4)–C(5)	127.3(3)
C(2)–C(3)–C(4)	122.2(4)	C(3)–C(4)–C(5)	116.2(4)

crystallographic details and selected bond distances and angles are given in Tables 1 and 2, respectively. Complex **2** has a trigonal bipyramidal geometry with two PPh_3 and the allyl ligand at the equatorial positions and the Cl and CO ligands at the axial positions. The P(1)–Ru(1)–P(2) angle is 107.08(4)°. The allyl complex is in the endo form, in which the H on the central allylic carbon points toward the CO ligand, which is expected from the results of a recent theoretical analysis of similar allyl complexes.^{9b} The bond distances and angles associated with the $\text{Ru}(\eta^3\text{-allyl})$ unit are normal, compared with those of the reported ruthenium allyl complex $\text{Ru}(\eta^3\text{-CH}_2\text{CHCHPh})\text{Cl}(\text{CO})(\text{PPh}_3)_2$.^{9b}

It appears that insertion reactions of $\text{RuHCl}(\text{CO})(\text{PPh}_3)_3$ with allenens always give allyl complexes, whether the substituents of allenens are electron-withdrawing or electron-donating. In order to see the effect of metal on the insertion reactions, we have studied the reactions of the closely related hydride complex $\text{OsHCl}(\text{CO})(\text{PPh}_3)_3$ (**3**) with $\text{CH}_2=\text{C}=\text{CHR}$ (*R* = Ph, CH_2Ph). Treatment of $\text{OsHCl}(\text{CO})(\text{PPh}_3)_3$ with $\text{CH}_2=\text{C}=\text{CHPh}$ produced the analogous allyl complex $\text{Os}(\eta^3\text{-CH}_2\text{CHCHPh})\text{Cl}(\text{CO})(\text{PPh}_3)_2$ (**4**) (eq 3).

The structure of **4** has also been confirmed by X-ray diffraction studies. The molecular structure of **4** is depicted in Figure 2, and selected bond distances and angles are given in

(20) Xue, P.; Zhu, J.; Sung, H. S. Y.; Williams, I. D.; Lin, Z.; Jia, G. *Organometallics* **2005**, *24*, 4896.

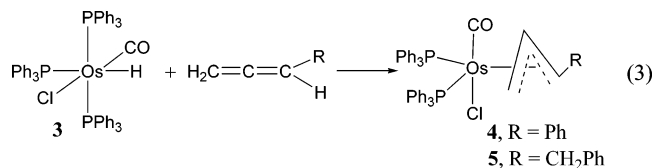


Table 3. The structure of complex **4** can be described as a trigonal bipyramid with two PPh₃ and the allyl ligand at the equatorial positions and the Cl and CO ligands at the axial positions. The P(1)–Os(1)–P(2) angle is 103.39(2)°. Like complexes RuCl(η^3 -allyl)(CO)(PR₃)₂, the osmium allyl complex is in the endo form, in which the hydrogen on the central allylic carbon points toward the CO ligand. The allyl ligand is coordinated to osmium in an unsymmetrical fashion, with the Os–C(central) bond (2.221(3) Å) being slightly shorter than the Os–C(terminal) bonds (2.245(3), 2.304(2) Å). The C–C and Os–C bond distances associated with the Os(η^3 -allyl) unit are similar to those of reported osmium allyl complexes, for example, CpOs(η^3 -CH₂CHCPh)(PⁱPr₃)₂,²¹ CpOs(η^3 -CH₂-CHCHCH₂Ph)(PⁱPr₃)₂,²² (C₅H₄SiPh₃)Os(η^3 -CH₂CPhCH₂)(Pⁱ-Pr₃)₂²³ and [Cp*Os(Me)(H₂O)(CH₂C(Me)CH₂)]BF₄.²⁴

Consistent with the X-ray structure, the ³¹P{¹H} NMR spectrum of **4** at room temperature (298.7 K) showed two signals at 5.2 and –5.2 ppm, due to the unsymmetrical nature of the allyl ligand. In the ¹H NMR spectrum, the allylic proton signals were observed at 3.19 (CH₂), 3.29 (CH₂), 4.27 (CHPh), and 5.79 (central CH) ppm.

Reported complexes closely related to **4** include the TBP allyl complexes Os(η^3 -C₃H₅)Cl(CO)(PⁱPr₃)₂,²⁵ OsH(η^3 -C₃H₅)(CO)-(PR₃)₂ (PR₃ = PⁱPr₃, PMe^tBu₂),²⁶ OsH(η^3 -CH₂CRCH₂)(CO)-(PPh₃)₂ (R = H, CH₃),²⁷ and [OsH(η^3 -PhCHCHCPh)(CO)₂-(PⁱPr₃)₂]BF₄.²⁸ The complexes Os(η^3 -C₃H₅)Cl(CO)(PⁱPr₃)₂ and OsH(η^3 -CH₂C(Me)CH₂)(CO)(PPh₃)₂ have a structure similar to **4**, in which the two PR₃ ligands are in the equatorial positions of the TBP structure. In complexes OsH(η^3 -C₃H₅)(CO)(PR₃)₂ (PR₃ = PⁱPr₃, PMe^tBu₂)²⁶ and [OsH(η^3 -PhCHCHCPh)(CO)₂-(PⁱPr₃)₂]BF₄,²⁸ the two PR₃ ligands are trans to each other and both in the axial positions. However, in OsH(η^3 -CH₂CHCH₂)(CO)(PPh₃)₂, the two PPh₃ ligands are cis to each other. One is in the axial position, and the other one is in the equatorial position.

Treatment of OsHCl(CO)(PPh₃)₃ with CH₂=C=CHCH₂Ph also gave the analogous allyl complex Os(η^3 -CH₂CHCH₂-Ph)Cl(CO)(PPh₃)₂ (**5**) (eq 3). Complex **5** must have a structure similar to that of **4**, as judged on the basis of the spectroscopic data. In particular, the ³¹P NMR spectrum of **5** shows two signals at 0.2 and 5.1 ppm, due to the unsymmetrical nature of the allyl ligand. The ¹³C{¹H} NMR spectrum displays signals associated with η^3 -CH₂CHCH₂Ph at 40.1 (s, CH₂Ph), 58.7 (=CH₂), 69.0 (CHCH₂Ph), and 98.0 (s, CH₂=CH) ppm.

Insertion Reactions of Allenes with MHCl(PPh₃)₃ (M = Ru, Os) Forming Vinyl Complexes. We have previously

(21) Esteruelas, M. A.; Gonzalez, A. I.; Lopez, A. M.; Olivan, M.; Onate, E. *Organometallics* **2006**, *25*, 693.

(22) Esteruelas, M. A.; González, A. I.; López, A. M.; Oñate, E. *Organometallics* **2003**, *22*, 414.

(23) Baya, M.; Esteruelas, M. A.; Onate, E. *Organometallics* **2001**, *20*, 4875.

(24) Mui, H. D.; Brumaghin, J. L.; Gross, C. L.; Girolami, G. S. *Organometallics* **1999**, *18*, 3264.

(25) Werner, H.; Stuer, W.; Wolf, J.; Laubender, M.; Weberndorfer, B.; Herbst-Irmer, R.; Lehmann, C. *Eur. J. Inorg. Chem.* **1999**, 1889.

(26) Schlunken, C.; Werner, H. *J. Organomet. Chem.* **1993**, *454*, 243.

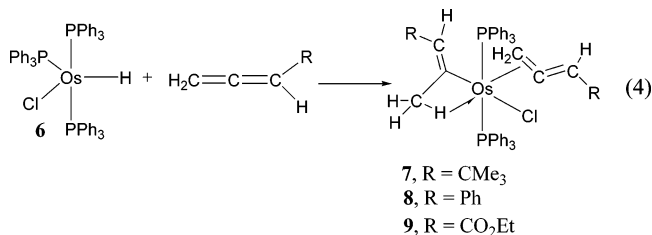
(27) Conway, C.; Kemmit, R. D. W.; Platt, A. W. G.; Russel, D. R.; Sherry, L. J. S. *J. Organomet. Chem.* **1985**, *292*, 419.

(28) Buil, M. L.; Esteruelas, M. A.; López, A. M.; Oñate, E. *Organometallics* **1997**, *16*, 3169.

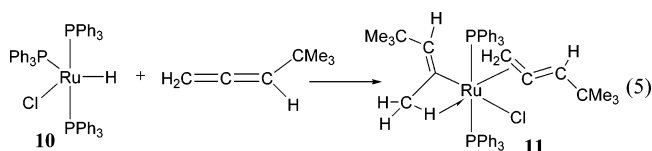
Table 3. Bond Lengths (Å) and Angles (deg) for Os(η^3 -CH₂CHCPh)Cl(CO)(PPh₃)₂ (4**)**

Os(1)–C(10)	1.857(3)	Os(1)–C(2)	2.221(3)
Os(1)–C(1)	2.245(3)	Os(1)–C(3)	2.304(2)
Os(1)–P(2)	2.3816(7)	Os(1)–P(1)	2.3837(7)
Os(1)–Cl(1)	2.4657(6)	O(1)–C(10)	1.132(3)
C(1)–C(2)	1.409(4)	C(2)–C(3)	1.416(4)
C(3)–C(4)	1.482(4)		
C(10)–Os(1)–C(1)	97.34(11)	C(10)–Os(1)–C(2)	81.47(11)
C(10)–Os(1)–C(3)	95.84(10)	C(10)–Os(1)–P(1)	85.50(8)
C(10)–Os(1)–P(2)	97.04(8)	C(10)–Os(1)–Cl(1)	179.45(8)
C(1)–Os(1)–C(2)	36.78(9)	C(1)–Os(1)–C(3)	66.36(9)
C(1)–Os(1)–P(1)	94.18(7)	C(1)–Os(1)–P(2)	158.06(8)
C(1)–Os(1)–Cl(1)	82.12(8)	C(2)–Os(1)–C(3)	36.42(10)
C(2)–Os(1)–P(1)	125.51(7)	C(2)–Os(1)–P(2)	130.57(7)
C(2)–Os(1)–Cl(1)	98.05(7)	C(3)–Os(1)–P(1)	160.53(7)
C(3)–Os(1)–P(2)	95.74(7)	C(3)–Os(1)–Cl(1)	83.89(7)
P(1)–Os(1)–P(2)	103.39(2)	P(1)–Os(1)–Cl(1)	94.58(2)
P(2)–Os(1)–Cl(1)	83.47(2)	C(2)–C(1)–Os(1)	70.66(15)
C(1)–C(2)–C(3)	123.6(3)	C(1)–C(2)–Os(1)	72.56(14)
C(3)–C(2)–Os(1)	75.01(15)	C(2)–C(3)–C(4)	121.4(2)
C(2)–C(3)–Os(1)	68.58(14)	C(4)–C(3)–Os(1)	125.94(17)

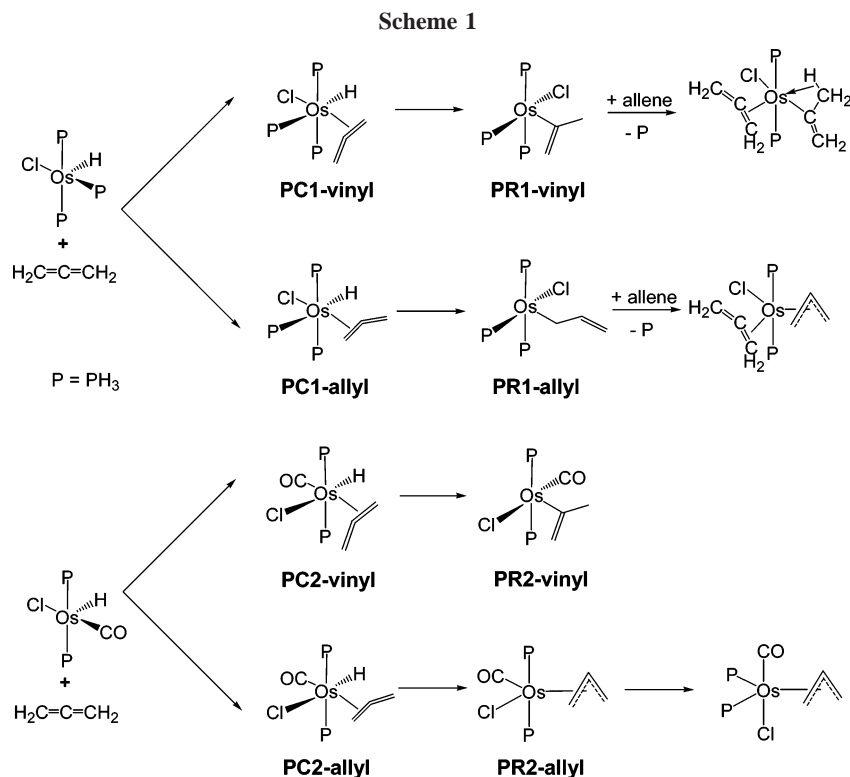
shown that reactions of OsHCl(PPh₃)₃ (**5**) with CH₂=C=CHR (R = CMe₃, Ph, CO₂Et) gave the vinyl complexes OsCl-(C(CH₃)=CHR)(CH₂=C=CHR)(PPh₃)₂ (**7**, R = CMe₃; **8**, R = Ph, **9**, R = CO₂Et) (eq 4).²⁰ The results described in the previous section clearly show that OsHCl(CO)(PPh₃)₃ behaves similarly to RuHCl(CO)(PPh₃)₃: their reactions with allenes always give η^3 -allyl complexes, suggesting that ligands play a very important role in determining the reaction pathways. By analogy with the reactions of MHCl(CO)(PPh₃)₃ with allenes, one might expect that RuHCl(PPh₃)₃, like OsHCl(PPh₃)₃, reacts with allenes to give vinyl complexes. To test this hypothesis, we have studied the reactions of RuHCl(PPh₃)₃ with allenes.



Indeed, the vinyl complex **11** was isolated from the reaction of the ruthenium complex RuHCl(PPh₃)₃ (**10**) with CH₂=C=CHCMe₃ (eq 5). We have also carried out reactions of RuHCl-(PPh₃)₃ (**10**) with other allenes, such as CH₂=C=CHPh, and CH₂=C=CHCO₂Et. Unfortunately, these reactions produced a mixture of species, and we have not been able to separate and fully characterize these products.



The structure of complex **11** can be readily assigned on the basis of the NMR spectroscopic data. The ³¹P{¹H} NMR spectrum of **11** in CD₂Cl₂ showed a singlet at 22.0 ppm. The ¹H NMR spectrum displayed the =CH₂ signal at 0.30 ppm and two =CH signals at 4.53 and 5.85 ppm. The presence of a β -agostic interaction is indicated by the observation of a methyl proton signal at 0.13 ppm. The chemical shift is unusually upfield for a typical CH₃ group attached to an sp²-hybridized carbon but is close to that of the methyl group with an agostic interaction in [IrPh(C(CH=CHCMe₃)=CHCMe₃)(PMe₃)₃]PF₆



(-0.7 ppm).²⁹ The ^1H NMR data of **11** are similar to those of complex **7**, which has been characterized structurally.

Theoretical Studies. The insertion reactions of allenes with $\text{MHCl}(\text{CO})(\text{PPh}_3)_3$ and $\text{MHCl}(\text{PPh}_3)_3$ presumably proceed through similar intermediates $\text{MHCl}(\eta^2\text{-allene})(\text{L})(\text{PPh}_3)_2$ ($\text{L} = \text{CO}, \text{PPh}_3$), but lead to very different products as described above. In order to better understand the results, density functional theory calculations were carried out on the model reactions shown in Scheme 1. Energetic calculations of the model reactions allow us to delineate how a different ligand environment influences the reaction products. The ligand arrangement of the $\text{OsHCl}(\text{CO})(\text{PPh}_3)_2$ metal fragment in the **PC2** intermediates is the same as that used in an early study on acetylene insertion in $\text{MHCl}(\eta^2\text{-acetylene})(\text{CO})(\text{PPh}_3)_2$.³⁰

The potential energy profiles, calculated for the formation of the vinyl (**PR1-vinyl**) and allyl (**PR1-allyl**) model complexes from $\text{OsHCl}(\eta^2\text{-allene})(\text{PPh}_3)_3$ (**PC1**), have been briefly mentioned in a preliminary report and are reproduced in Figure 3. The results indicate that the pathway leading to the formation of the vinyl complex **PR1-vinyl** is kinetically more favorable. The high barrier for the reverse process, **PR1-vinyl** \rightarrow **PC1-vinyl**, prevents the observation of the thermodynamically more stable η^3 -allyl complex. An important implication of the results is that although vinyl complexes are in general thermodynamically less stable than η^3 -allyl complexes (in view of the dominant allyl complexes in the literature), formation of vinyl complexes is still kinetically possible. $\text{OsHCl}(\text{PPh}_3)_3$ provides an example for such a possibility to be realized.

The potential energy profiles, calculated for the formation of the vinyl (**PR2-vinyl**) and allyl (**PR2-allyl**) model complexes from $\text{OsHCl}(\eta^2\text{-allene})(\text{CO})(\text{PPh}_3)_2$ (**PC2**), are shown in Figure 4. Overall, the reaction barriers are smaller than those for the reactions of $\text{OsHCl}(\eta^2\text{-allene})(\text{PPh}_3)_3$ (**PC1**). The pathway leading to the formation of the η^3 -allyl complex is found to be both

kinetically and thermodynamically more favorable, although the **TS2-allyl** is not significantly lower in energy than **TS2-vinyl**. Different from **TS1-allyl**, **TS2-allyl** does not connect the precursor complex **PC2-allyl** with an η^1 -allyl species similar to **PR1-allyl**, but with the η^3 -allyl species **PR2-allyl**. The difference is probably related to the fact that the $\text{Os}-\text{CO}$ bond in **TS2-allyl** is more rigid than the corresponding $\text{Os}-\text{P}$ bond in **TS1-allyl**.

To study the steric effect missed from the small model calculations, we also carried out two-layer ONIOM calculations with the real PPh_3 ligands for all the species in Figure 4 (see the data in italics) and the two transition state structures in Figure 3. From Figure 4, we can see that the PPh_3 and PH_3 results are similar, in particular for the **PC** and **TS** species. When PPh_3 is used, **PR2-vinyl** is relatively more stable and **PR2-allyl** becomes relatively destabilized. The results are expected because the former is five-coordinate and the latter is six-coordinate with a sterically demanding η^3 -allyl ligand. The final product in which the two PPh_3 ligands are cis to each other is relatively destabilized even more because of the cis arrangement of the two bulky PPh_3 ligands. The energy difference between **TS1-allyl** and **TS1-vinyl** shown in Figure 3 is 2.5 kcal/mol in free energy and 2.1 kcal/mol in electronic energy. When PPh_3 is used, both **TS1-allyl** and **TS1-vinyl** are relatively destabilized by ca. 2–3 kcal/mol, and the energy difference between them becomes 2.5 kcal/mol in free energy and 3.2 kcal/mol in electronic energy. All these additional ONIOM calculations suggest that the PH_3 results are qualitatively correct. The qualitative reliability of the PH_3 results is understandable because the steric effect of the PPh_3 ligands is similar for the reactants and the transition states.

Earlier theoretical studies show that olefin insertion into an $\text{M}-\text{R}$ bond is kinetically and thermodynamically less favorable when a metal(d)-to-olefin(π^*) back-bonding interaction is present.³¹ The back-bonding interaction makes the olefin carbons "electron-rich", leading to a high activation barrier for the migration of the alkyl ligand to form the new $\sigma_{\text{C}-\text{R}}$ bond. This

(29) Selnau, H. E.; Merola, J. S. *J. Am. Chem. Soc.* **1991**, *113*, 4008.

(30) Marchenko, A. V.; Gerard, H.; Eisenstein, O.; Caulton, K. G. *New J. Chem.* **2001**, *25*, 1244.

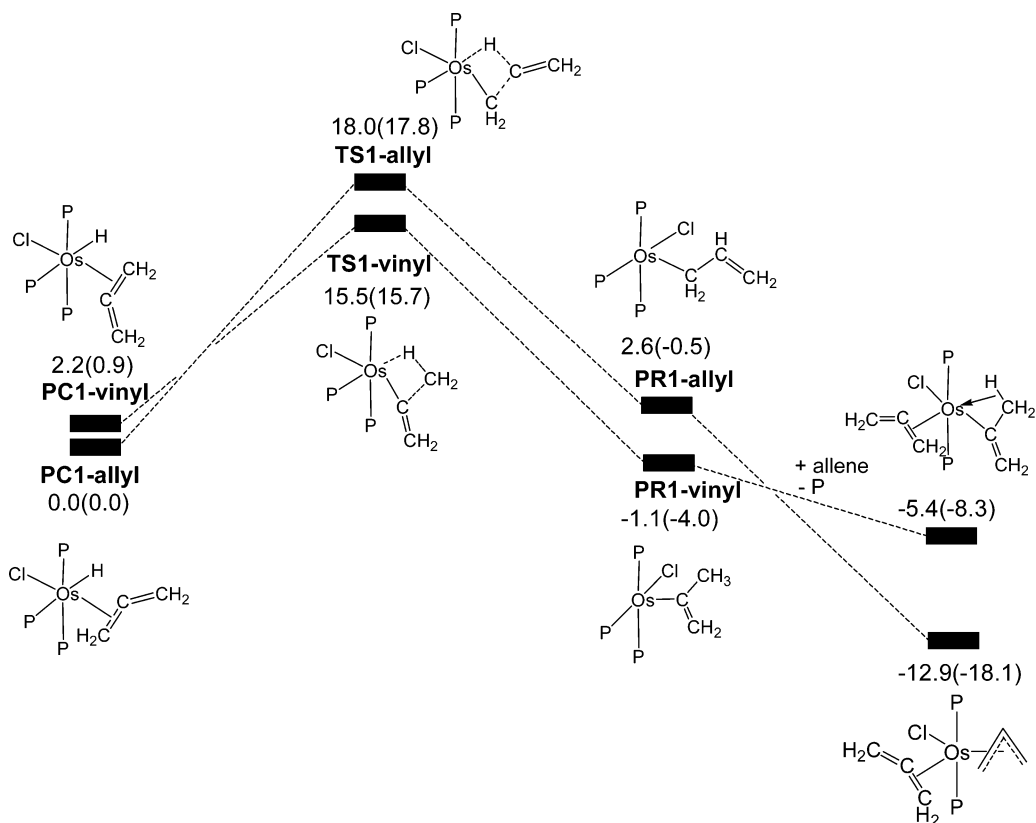


Figure 3. Energy profiles of the two possible insertion pathways calculated for $\text{OsHCl(allyl)(PPh}_3)_3$. P stands for PH_3 used in the calculations. The calculated relative free energies and electronic energies (in parentheses) are given in kcal/mol.

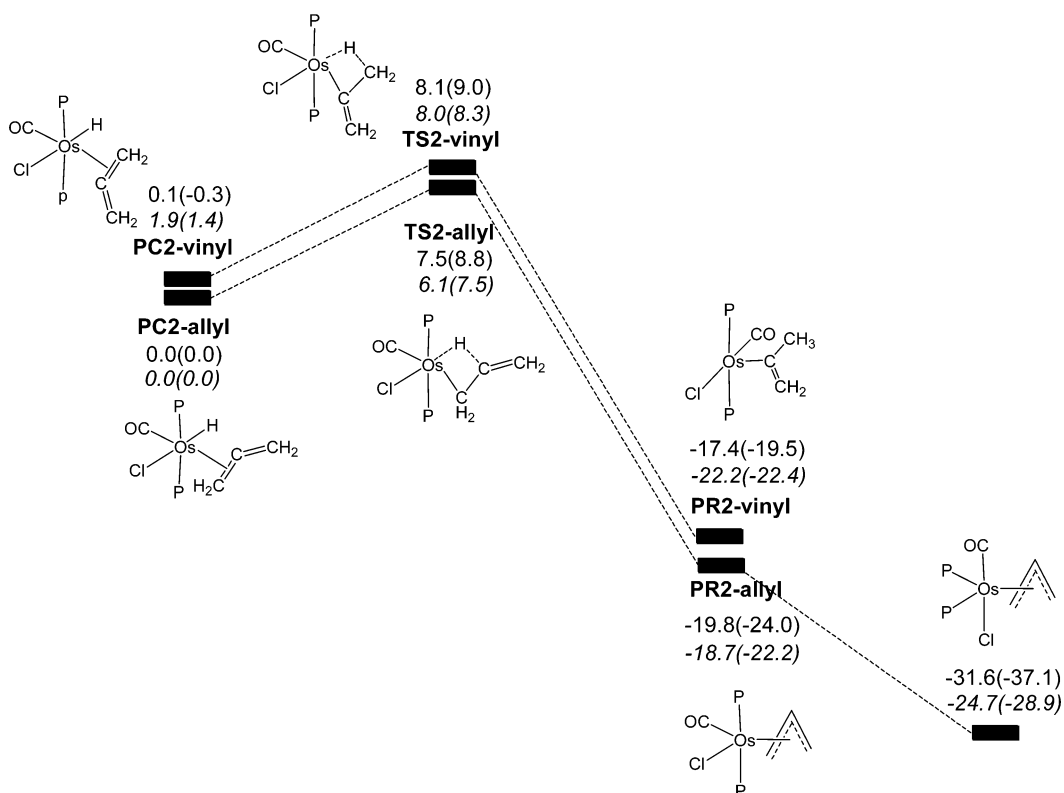


Figure 4. Energy profiles of the two possible insertion pathways calculated for $\text{OsHCl(allyl)(CO)(PPh}_3)_2$. P stands for PH_3 used in the calculations. The calculated relative free energies and electronic energies (in parentheses) are given in kcal/mol. Two sets of energy data are given. The first set was obtained from the calculations using PH_3 as the model phosphine ligand. The second set (in italics) was obtained from the ONIOM calculations considering the steric effect of the PPh_3 ligands.

early finding explains why the insertion pathways of $\text{OsHCl-}(\eta^2\text{-allene})(\text{CO})(\text{PH}_3)_2$ have lower barriers than those of OsHCl-

$(\eta^2\text{-allene})(\text{PH}_3)_3$. The presence of the CO ligand makes the back-bonding interaction relatively weaker, as evidenced by the

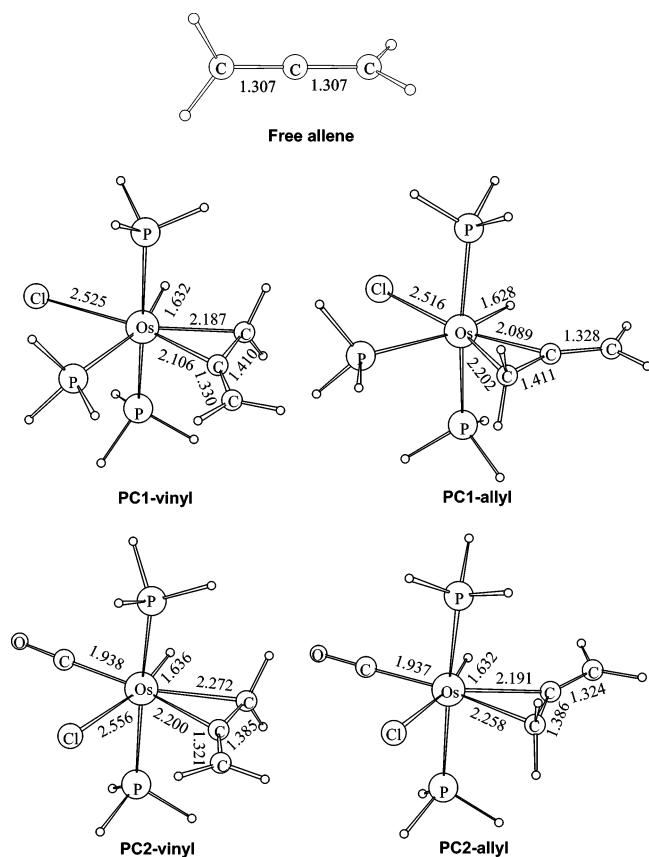


Figure 5. Calculated structures of $OsHCl(allene)(PH_3)_3$ and $OsHCl(allene)(CO)(PH_3)_2$.

longer metal–carbon(allene) bond distances in **PC2-vinyl** and **PC2-allyl** when compared to those in **PC1-vinyl** and **PC1-allyl** (Figure 5).

The preferred insertion reaction pathways of $OsHCl(\eta^2\text{-allene})(CO)(PH_3)_2$ (**PC2**) and $OsHCl(\eta^2\text{-allene})(PH_3)_3$ (**PC1**) are clearly reversed. The theoretical calculations accurately reproduce the trend observed experimentally. Replacement of one phosphine ligand by a carbonyl ligand drastically changes the preferred insertion reaction pathways. A plausible explanation of the above-mentioned calculation results is given below.

In allene insertion into a $M-H$ bond, a hydride migrates to the allene ligand to form a new $C-H$ bond. Therefore, it is a reasonable assumption that the migratory hydride looks for a carbon center that is more electron-deficient. The central carbon of a free allene is especially electron-deficient when compared with the two terminal carbons (see Figure 6 for the charge distribution of a free allene). Thus one would expect that a nucleophile such as a hydride will normally attack the central carbon. However, when an allene is η^2 -coordinated to a metal center, the charge distribution will be altered due to the metal–allene interaction. The metal(d)-to-allene(π^*) back-donation is expected to be much more significant between the metal center and the central carbon of the allene ligand.

The charge distribution shown in Figure 6, obtained from the Mulliken population analysis using both ECP and all-electron basis sets, indeed indicates that from a free allene to a coordinated allene, the central carbon of the allene in each precursor complex gains electrons while the terminal carbons lose electrons upon coordination. The gain of electrons by the central carbon of allene is so significant for the complex **PC1**

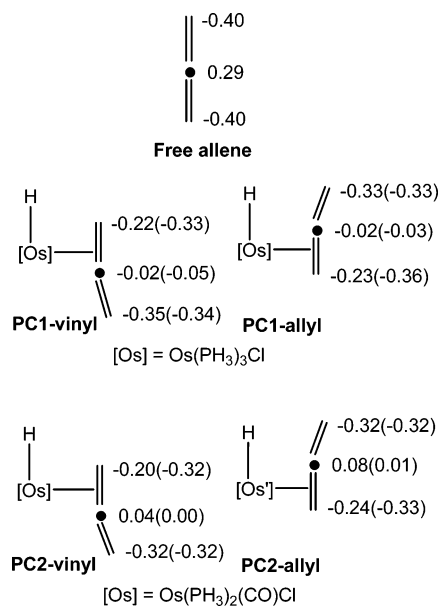


Figure 6. Atomic charges obtained from Mulliken population analysis using both the ECP and all-electron (in parentheses) basis sets.

with a more electron-rich metal center that the charge of the central carbon of allene changes from positive in the free allene to negative in the allene complex. The calculated structures of the precursor complexes (Figure 5) also show that in each complex the metal center has a shorter $Os-C$ bond with the central carbon of the allene ligand. Because of the difference in the degree of back-bonding interactions from the metal center to the central carbon and to the terminal carbons, we have the following two scenarios: (1) the back-donation to allene is not significant enough, so that the migration of the hydride to the central carbon is still more favorable; (2) the back-donation to allene is significant enough to make the migration of the hydride to the central carbon less favorable. The first scenario is apparently more prevalent in view of the fact that insertion reactions of Allenes with L_nM-R normally give allyl complexes. Clearly, that insertion of allene into the $Os-H$ bond in $OsHCl(PPh_3)_3$ gives a vinyl product observed experimentally provides an example for the latter scenario.

Figure 6 shows that upon coordination the central carbon of the allene ligand in **PC1** gains more electrons than the central carbon of the allene ligand in **PC2**. The significant difference in the electron density increase at the central carbon of the allene ligand upon coordination between the two precursor complexes leads to the reactivity difference observed. The back-donation is less significant in **PC2** due to the presence of the strong π -accepting CO ligand. At first glance of the charge distribution in **PC1** and **PC2** shown in Figure 6, one may have the feeling that **PC1** should also evolve to an allyl complex, as the central carbon is still less electron-rich than the terminal ones. In Figure 6, the partial atomic charges represent the charges derived from both σ and π components. However, we expect that it is the π -electron density, which is more significantly affected by back-donation, that determines the regiochemistry. Computationally, we have difficulty in separating the π component from the σ component. The data given in Figure 6 are intended to show the qualitative trend in order to support the plausible explanation and should not be taken as a criterion to understand the reverse regiochemistry observed experimentally.

Conclusion. Allene insertion reactions with $MHCl(PPh_3)_3$ and $MH(CO)(PPh_3)_3$ ($M = Ru, Os$) have been carefully investigated.

(31) Margl, P.; Deng, L.; Ziegler, T. *J. Am. Chem. Soc.* **1998**, *120*, 5517. Niu, S.; Hall, M. B. *Chem. Rev.* **2000**, *100*, 353.

It was found that $\text{MHCl}(\text{PPh}_3)_3$ reacts with allenes to give vinyl complexes, while $\text{MHCl}(\text{CO})(\text{PPh}_3)_3$ reacts with allenes to give η^3 -allyl complexes. To understand the difference, allene insertion reactions involving $\text{OsHCl}(\text{PPh}_3)_3$ and $\text{OsHCl}(\text{CO})(\text{PPh}_3)_3$ have also been investigated by computational chemistry. On the basis of the computational results, the following plausible explanation is given. Since the central carbon of free allene is electron-deficient when compared with the two terminal carbons, insertion of allene into a metal–hydride will normally give an allyl complex. However, when an allene is η^2 -coordinated to a metal fragment, the charge distribution will be altered due to the metal–allene interaction. In particular, the metal(d)-to-allene(π^*) back-donation is much more significant between the metal center and the central carbon of the allene ligand. Thus insertion reactions involving a more electron-rich metal center could give vinyl complexes rather than the usual allyl complexes. To test the scope and limitation of this explanation, we will carry out experiments involving varieties of allenes, metals, and ligands.

Experimental Section

All manipulations were carried out under a nitrogen atmosphere using standard Schlenk techniques unless otherwise stated. Solvents were distilled under nitrogen from sodium benzophenone (hexane, ether, THF), sodium (benzene), or calcium hydride (CH_2Cl_2). The starting materials $\text{OsHCl}(\text{PPh}_3)_3$,³² $\text{RuHCl}(\text{PPh}_3)_3$,³³ $\text{RuHCl}(\text{CO})(\text{PPh}_3)_3$,³⁴ $\text{OsHCl}(\text{CO})(\text{PPh}_3)_3$,³⁴ 4,4-dimethyl-1,2-pentadiene,³⁵ phenylallene,³⁵ $\text{CH}_2=\text{C}=\text{CHCO}_2\text{Me}$,³⁵ and $\text{CH}_2=\text{C}=\text{CHCH}_2\text{Ph}$ ³⁵ were prepared following the procedures described in the literature. All other reagents were used as purchased from Aldrich Chemical Co.

Microanalyses were performed by M-H-W Laboratories (Phoenix, AZ) or collected on a VARIO EL III analyzer at Shanghai Institute of Organic Chemistry. ^1H , $^{13}\text{C}\{^1\text{H}\}$, and $^{31}\text{P}\{^1\text{H}\}$ spectra were collected on a Varian Mercury spectrometer (300 MHz) or a Bruker ARX-300 spectrometer (300 MHz). ^1H and ^{13}C NMR shifts are relative to TMS, and ^{31}P chemical shifts are relative to 85% H_3PO_4 .

$\text{Ru}(\eta^3\text{-CH}_2\text{CHCHCO}_2\text{Me})\text{Cl}(\text{CO})(\text{PPh}_3)_2$ (2). A mixture of $\text{RuHCl}(\text{CO})(\text{PPh}_3)_3$ (143 mg, 0.15 mmol) and methyl buta-2,3-dienoate (29 mg, 0.30 mmol) in dichloromethane (6 mL) was stirred at room temperature for 15 min to give a clear green solution. The resulting solution was concentrated to dryness under vacuum, and the oily residue was treated with ether (25 mL) to give a pale yellow solid. The solid was collected by filtration, washed with ether (25 mL), and dried under vacuum. Yield: 115 mg, 83%. ^1H NMR (300 MHz, CDCl_3): δ 2.94–3.00 (m, 1 H, CHCO_2Me), 3.06–3.20 (m, 2 H, $\text{CH}_2=$), 3.10 (s, OCH_3), 5.75–5.86 (m, 1 H, $\text{C}=\text{CHC}$), 7.19–7.40 (m, 26 H, Ph), 7.47–7.53 (m, 4 H, Ph). $^{31}\text{P}\{^1\text{H}\}$ NMR (121.5 MHz, CDCl_3): δ 28.9 (d, $J(\text{PP}) = 10.9$ Hz), 39.5 (d, $J(\text{PP}) = 10.9$ Hz). $^{13}\text{C}\{^1\text{H}\}$ NMR (75.47 MHz, CDCl_3): δ 51.7 (s, OCH_3), 60.7 (d, $J(\text{PC}) = 28.2$ Hz, CH), 67.8 (d, $J(\text{PC}) = 21.9$ Hz, CH_2), 103.5 (s, CH), 127.5–134.8 (m, Ph), 174.7 (d, $J(\text{PC}) = 2.8$ Hz, CO), 200.0 (dd, $J(\text{PC}) = 16.5$, 11.8 Hz, CO). Anal. Calcd for $\text{C}_{42}\text{H}_{37}\text{ClO}_3\text{P}_2\text{Ru}$: C, 64.00; H, 4.73. Found: C, 63.31; H, 4.77. As indicated by ^1H NMR, the sample contains ca. 15 mol % dichloromethane. Anal. Calcd for $\text{C}_{42}\text{H}_{37}\text{ClO}_3\text{P}_2\text{Ru}\cdot 0.15\text{CH}_2\text{Cl}_2$: C, 63.21; H, 4.69.

$\text{Os}(\eta^3\text{-CH}_2\text{CHCHPh})\text{Cl}(\text{CO})(\text{PPh}_3)_2$ (4). To a suspension of $\text{OsHCl}(\text{CO})(\text{PPh}_3)_3$ (215 mg, 0.207 mmol) in dichloromethane (8 mL) was added a solution of phenylallene (70 mg, 0.60 mmol) in hexane (0.3 mL). After the resulting mixture was stirred for 14 h, the solution was filtered, the filtrate was concentrated to dryness under vacuum, and the oily residue was treated with ether (2 mL) to give a solid. The solid was then redissolved in benzene (5 mL). After filtration, the filtrate was concentrated to dryness and the residue was washed with hexane and dried under vacuum to give a yellow solid. Yield: 86 mg, 48%. ^1H NMR (300 MHz, C_6D_6 , 298 K): δ 3.19 (dd, $J(\text{PH}) = 4.5$ Hz, $J(\text{HH}) = 11.7$ Hz, 1 H, $=\text{CH}_2$), 3.29 (m, 1 H, $=\text{CH}_2$), 4.27 (dd, $J(\text{PH}) = 5.7$ Hz, $J(\text{HH}) = 11.2$ Hz, 1 H, CHPh), 5.79 (m, 1 H, $\text{C}=\text{CHC}$), 7.06–7.24 (m, 23 H, CH-Ph , P-Ph), 7.74–7.88 (m, 12 H, P-Ph). $^{31}\text{P}\{^1\text{H}\}$ NMR (121.5 MHz, C_6D_6 , 298 K): δ 5.2 (s), –5.2 (s). Anal. Calcd for $\text{C}_{46}\text{H}_{39}\text{ClO}_3\text{OsP}_2$: C, 61.70; H, 4.39. Found: C, 61.90; H, 4.55.

$\text{Os}(\eta^3\text{-CH}_2\text{CHCHCH}_2\text{Ph})\text{Cl}(\text{CO})(\text{PPh}_3)_2$ (5). A mixture of $\text{OsHCl}(\text{CO})(\text{PPh}_3)_3$ (200 mg, 0.19 mmol) and buta-2,3-dienylbenzene (74 mg, 0.57 mmol) in dichloromethane (15 mL) was stirred for 2 days at room temperature to give a clear yellow solution. The resulting solution was concentrated to dryness under vacuum. The oily residue was treated with ether (15 mL) to give a white solid, which was collected by filtration, washed with ether (3 \times 15 mL), and dried under vacuum. Yield: 63 mg, 35%. ^1H NMR (300 MHz, C_6D_6 , 298 K): δ 2.67–2.62 (m, 1 H, CH_2Ph), 2.96–2.80 (m, 2 H, 1 H of $\text{CH}_2=\text{CH}$ and 1 H of CH_2Ph), 3.03–2.96 (m, 1 H, $\text{CH}_2=\text{CH}$), 3.42–3.30 (m, 1 H, $\text{CH-CH}_2\text{Ph}$), 4.96 (dd, $J(\text{HH}) = 18.7$ Hz, $J(\text{PH}) = 10.8$ Hz, 1 H, $\text{C}=\text{CH-C}$), 7.15–6.85 (m, 24 H, $\text{CH}_2\text{-Ph}$, P-Ph), 7.61–7.55 (m, 6 H, P-Ph), 7.84–7.78 (m, 24 H, P-Ph). $^{31}\text{P}\{^1\text{H}\}$ NMR (121.5 MHz, C_6D_6): δ 0.19 (s), 5.08 (s). $^{13}\text{C}\{^1\text{H}\}$ NMR (75.4 MHz, C_6D_6): δ 40.1 (s, CH_2Ph), 58.7 (d, $J(\text{PC}) = 24.8$ Hz, $=\text{CH}_2$), 69.0 (d, $J(\text{PC}) = 27.1$ Hz, CHCH_2Ph), 98.0 (s, $\text{CH}_2=\text{C}$), 144.8–126.1 (m, Ph), 180.0 (t, $J(\text{PC}) = 8.9$ Hz, CO). Anal. Calcd for $\text{C}_{47}\text{H}_{41}\text{ClO}_3\text{OsP}_2$: C, 62.07; H, 4.54. Found: C, 61.83; H, 4.63.

$\text{Ru}(\text{C}(\text{CH}_3)=\text{CHCMe}_3)(\eta^2\text{-1,2-CH}_2=\text{C}=\text{CHCMe}_3)\text{Cl}(\text{PPh}_3)_2$ (11). To a solution of $\text{RuHCl}(\text{PPh}_3)_3$ (308 mg, 0.333 mmol) in dichloromethane (8 mL) was added dropwise a solution of 4,4-dimethyl-1,2-pentadiene (65 mg, 0.67 mmol) in pentane (0.5 mL) at room temperature. The resulting solution was allowed to stir for 7 h. After the mixture was concentrated to dryness, a paste was formed. Addition of diethyl ether (5 mL) to the residue produced a yellow solid, which was collected by filtration, washed with ether (3 mL \times 3), and dried under vacuum. Yield: 100 mg, 35%. ^1H NMR (300 MHz, CD_2Cl_2 , 298 K): δ 0.13 (s, 3 H, agostic CH_3), 0.30 (m, 2 H, CH_2), 0.68 (s, 9 H, CMe_3), 0.97 (s, 9 H, CMe_3), 4.53 (br s, 1 H, $\text{CH}=\text{C}$), 5.85 (br t, 1 H, $\text{CH}=\text{C}$), 7.16–7.32 (m, 18 H, Ph), 7.46–7.62 (m, 12 H, Ph). $^{31}\text{P}\{^1\text{H}\}$ NMR (121.5 MHz, CD_2Cl_2 , 298 K): δ 22.0 (s). Anal. Calcd for $\text{C}_{50}\text{H}_{55}\text{ClP}_2\text{Ru}$: C, 70.28; H, 6.49. Found: C, 70.12; H, 6.32.

Crystal Structure Analyses of 2 and 4. Crystals of **2** were grown from a CH_2Cl_2 solution of **2** layered with ether. The compound is sufficiently air stable, and a crystal of dimensions 0.36 \times 0.17 \times 0.06 mm³ was mounted on a glass fiber with epoxy adhesive. Crystals of **4** were grown from CH_2Cl_2 solutions of **4** layered with hexane. A crystal of dimensions 0.20 \times 0.15 \times 0.10 mm³ was selected for data collection. The diffraction intensity data were collected with a Bruker Smart APEX CCD diffractometer with graphite-monochromated Mo $\text{K}\alpha$ radiation ($\lambda = 0.71073$ Å) at 298 K for **2** and 100 K for **4**. Lattice determination and data collection were carried out using SMART v.5.625 software. Data reduction and absorption correction by empirical methods were performed using SAINT v 6.26 and SADABS v 2.03, respectively. Structure solution and refinement were performed using the SHELXTL v.6.10 software package. Both the structures were solved by direct methods, expanded by difference Fourier syntheses, and refined by full matrix least-squares on F^2 . All non-hydrogen atoms were

(32) Ferrando, G.; Caulton, K. G. *Inorg. Chem.* **1999**, *38*, 4168.

(33) Hallman, R. S.; McGarvey, B. R.; Wilkinson, G. *J. Chem. Soc. (A)* **1968**, 3143.

(34) Ahmad, N.; Levison, J. J.; Robinson, S. D.; Uttley, M. F.; Wonchoba, E. R.; Parshall, G. W. *Inorg. Synth.* **1974**, *15*, 45.

(35) (a) Brandsma, L.; Verkruijse, H. D. *Studies in Organic Chemistry 8, Synthesis of Acetylene, Allenes and Cumulenes*; Elsevier: Amsterdam, 1981. (b) Trost, B. M.; Pinkerton, A. B.; Seidel, M. *J. Am. Chem. Soc.* **2001**, *123*, 12466.

refined anisotropically with a riding model for the hydrogen atoms. Further details on crystal data and data collection and refinements parameters are summarized in Table 1.

Computational Details. Molecular geometries were optimized at the Becke3LYP (B3LYP) level of density functional theory.³⁶ Frequency calculations at the same level of theory have also been performed to identify all stationary points as minima (zero imaginary frequency). The effective core potentials (ECPs) of Hay and Wadt with a double- ζ valence basis sets (LanL2DZ)³⁷ were used to describe Os, P, and Cl atoms, while the standard 6-31G** basis set was used for C, O, and H atoms. Polarization functions were added for Cl ($\zeta(d) = 0.514$) and P ($\zeta(d) = 0.34$).³⁸ Calculations of intrinsic reaction coordinates (IRC)³⁹ were also performed on transition states to confirm that such structures are indeed connecting two minima. All the calculations were performed with the Gaussian 03 software package.⁴⁰

In order to test the reliability of the atomic charges obtained from the Mulliken population analysis on the basis of the ECP basis set utilized in the calculations, we also performed single-point SCF

(36) (a) Becke, A. D. *J. Chem. Phys.* **1993**, *98*, 5648. (b) Miehlich, B.; Savin, A.; Stoll, H.; Preuss, H. *Chem. Phys. Lett.* **1989**, *157*, 200. (c) Lee, C.; Yang, W.; Parr, G. *Phys. Rev. B* **1988**, *37*, 785.

(37) Hay, P. J.; Wadt, W. R. *J. Chem. Phys.* **1985**, *82*, 299.

(38) Huzinaga, S. *Gaussian Basis Sets for Molecular Calculations*; Elsevier Science Pub. Co.: Amsterdam, 1984.

(39) (a) Fukui, K. *J. Phys. Chem.* **1970**, *74*, 4161. (b) Fukui, K. *Acc. Chem. Res.* **1981**, *14*, 363.

(40) Frisch, M. J.; et al. *Gaussian 03*, revision B05; Gaussian, Inc.: Pittsburgh, PA, 2003.

calculations with Huzinaga's all-electron basis set (4322211/42211/4221/3)³⁸ for Os and 6-31G** for the rest of the atoms.

In our DFT calculations, we used PH_3 as a model for PPh_3 . To study the steric effect missed from the small model calculations, we performed two-layer ONIOM (B3LYP/BSI:HF/LanL2MB)⁴¹ calculations with the real PPh_3 ligand for several selected species. In the ONIOM calculations, the phenyl groups on the phosphine ligand were treated as the second layer while the rest were treated as the first layer. BSI represents the ECP basis set described above.

Acknowledgment. This work was supported by the National Natural Science Foundation of China through the Outstanding Young Investigator Award Fund (Project No. 20429201), the Hong Kong Research Grant Council (Project Nos. HKUST601804 and DAG05/06.SC19), and the Chinese Academy of Science.

Supporting Information Available: Complete ref 40 and Cartesian coordinates of the calculated structures (PDF). X-ray crystallographic files (CIF). This material is available free of charge via the Internet at <http://pubs.acs.org>.

OM700629X

(41) For references of the ONIOM method, see: (a) Dapprich, S.; Komáromi, I.; Byun, K. S.; Morokuma, K.; Frisch, M. J. *J. Mol. Struct. (THEOCHEM)* **1999**, *462*, 1. (b) Vreven, T.; Morokuma, K. *J. Comput. Chem.* **2000**, *21*, 1419. For a similar two-layer ONIOM calculation, see: (c) Ananikov, V. P.; Szilagyí, R.; Morokuma, K.; Musaev, D. G. *Organometallics* **2005**, *24*, 1938.